Finite-Time and -Size Scalings in the Evaluation of Large Deviation Functions Part II: Numerical Approach in Continuous Time

Esteban Guevara Hidalgo, Takahiro Nemoto, Vivien Lecomte

Finite-Time and -Size Scalings in the Evaluation of Large Deviation Functions Part II: Numerical Approach in Continuous Time

Esteban Guevara Hidalgo,[1,2,*] Takahiro Nemoto,[2] and Vivien Lecomte[2]

[1] *Institut Jacques Monod, CNRS UMR 7592, Université Paris Diderot, Sorbonne Paris Cité, F-750205, Paris, France*
[2] *Laboratoire de Probabilités et Modèles Aléatoires, Sorbonne Paris Cité, UMR 7599 CNRS, Université Paris Diderot, 75013 Paris, France*

(Dated: August 2, 2016)

Rare trajectories of stochastic systems are important to understand – because of their potential impact. However, their properties are by definition difficult to sample directly. Population dynamics provide a numerical tool allowing their study, by means of simulating a large number of copies of the system, which are subjected to a selection rule that favors the rare trajectories of interest. Such algorithms are plagued by finite simulation time- and finite population size- effects that can render their use delicate. In this second part of our study (which follows a companion paper [1] dedicated to an analytical study), we present a numerical approach which verifies and uses the finite-time and finite-size scalings of estimators of the large deviation functions associated to the distribution of the rare trajectories. Using the continuous-time cloning algorithm, we propose a method aimed at extracting the infinite-time and infinite-size limits of the estimator of such large deviation functions in a simple system, where, by comparing the numerical results to exact analytical ones, we demonstrate the practical efficiency of our proposed approach.

PACS numbers: 05.40.-a, 05.10.-a, 05.70.Ln

I. INTRODUCTION

Rare events and rare trajectories can be analyzed through a variety of numerical approaches, ranging from importance sampling [2], adaptive multilevel splitting [3] to transition path sampling [4] (see *e.g.* [5, 6] for reviews). In this paper, we focus on population dynamics algorithms, as introduced in [7, 8], which aims at studying rare trajectories by exponentially biasing their probability. This makes it possible to render typical the rare trajectories of the original dynamics in the simulated dynamics. The idea is to perform the numerical simulation of a large number of copies N_c of the original dynamics, supplemented with selection rules which favor the rare trajectories of interest.

Following the analytical study we proposed in a companion paper [1] (to which we will refer as 'Part I'), we consider a simple two-state numerical example, a creation-annihilation process, and we study trajectories with atypical activity, using the population dynamics algorithm in its continuous-time variant [9, 10]. Although the limitations and associated improvements of the population dynamics algorithm have been previously considered [11–14], in this article we study in depth the large-time and large-size scalings, aiming at improving the numerical evaluation of large deviation functions.

The version of the population dynamics algorithm introduced by Giardinà, Kurchan and Peliti [7] provides a method to evaluate the large deviation function (LDF) associated to the distribution of a trajectory-dependent observable. The LDF is obtained as the exponential growth rate that the population would present if it was not kept constant. Under this approach, the corresponding LDF estimator is in fact valid only in the limits of infinite simulation time t and infinite population size N_c. The usual strategy that is followed in order to obtain those limits is to increase the simulation time and the population size until the average of the estimator over several realizations does not depend on those two parameters, up to numerical uncertainties. Here on the other hand, (as announced in Part I) we propose a method that takes into account the exact scaling of the finite-time and finite-size corrections in order to extract the asymptotic limit of the estimator in the infinite-time and infinite-size limits.

The paper is organized as follows. In Sec. II we define the large deviations of our additive observable of interest and we detail how they can be estimated using the continuous-time population dynamics algorithm. In Sec. III we study the behavior of this estimator as a function of the duration of the observation time at fixed population. We extract its infinite-time limit and additionally we study its distribution and its associated large deviations. In Sec. IV we analyze the behavior of the estimator as we increase the number of clones for a (given) fixed simulation time. Based on these results, we present in Sec. V a method which allows us to extract the infinite-time, infinite-size limit of the large deviation function from a finite-time, finite-size scaling analysis. We complement these results by studying in Sec. VI an alternative way of defining the LDF estimator and finally, we gather our conclusions in Sec. VII.

* esteban_guevarah@hotmail.com; nemoto@math.univ-paris-diderot.fr; vivien.lecomte@univ-paris-diderot.fr

II. CONTINUOUS-TIME CLONING ALGORITHM

A. Large Deviations of Additive Observables

We consider a general Markov process on a discrete space of configurations $\{C\}$, with transition rates $W(C \to C')$. A trajectory of configurations generated in this process is denoted by $(C_0, \dots, C_K)$ starting from C_0 and presenting K jumps occurring at times $(t_k)_{1\le k\le K}$. We denote by $C(t')$ the state of the system at time t': when $t_k \le t' < t_{k+1}$, $C(t') = C_k$ $(k = 0, 1, 2, \cdots K-1)$ with $t_0 = 0$. We are especially interested in the large deviations of additive observables of trajectories of fixed duration t, of the form

$$\mathcal{O} = \sum_{k=1}^{K-1} a(C_k, C_{k+1}) + \int_0^t dt'\, b(C(t')), \tag{1}$$

where the functions a and b describe the elementary increments of the observables: a accounts for quantities associated with transitions (of state), whereas b does for static quantities. A simple example of observables of this form is that of the activity $\mathcal{O} = K$, which is the number of configuration changes on the time interval $[0, t]$ (in this case one has $a(C, C') = 1$ and $b \equiv 0$). We denote the joint distribution function of the state C and these observables $\mathcal{O}$ at time t by $P(C, \mathcal{O}, t)$.

In order to analyze large deviations of these additive observables, we follow the standard procedure as explained for example in [9, 10]. For this, we consider the moment generating function

$$Z(s, t) = \langle e^{-s\mathcal{O}} \rangle, \tag{2}$$

where $\langle\cdot\rangle$ means the expected value with respect to trajectories. Since the observables $\mathcal{O}$ are additive and the system is described by a Markov process, $Z(s, t)$ satisfies at large times the scaling

$$Z(s, t) \sim e^{t\psi(s)} \quad \text{for } t \to \infty, \tag{3}$$

where $\psi(s)$ is the growth rate of $Z(s, t)$ with respect to time. This exponent, known as the scaled cumulant generating function (CGF), is the quantity of interest in this paper. It allows us to recover the large-time limit of the cumulants of $\mathcal{O}$ as derivatives of $\psi(s)$ in $s = 0$, and more generically, the distribution of $\mathcal{O}/t$ from the Legendre transform of $\psi(s)$ [15] known as a (large deviation) rate function (see also Part I). Hereafter, we use the term "large deviation function" to refer both to the CGF and to the rate function, because these two are equivalent in systems that do not show any phase transition.

B. The Mutation-Selection Mechanism

The moment generating function $Z(s, t)$ can be computed numerically using the cloning algorithm [7, 8]. In order to do that, we introduce the Laplace transform of the probability distribution $P(C, \mathcal{O}, t)$, defined as

$$\hat{P}(C, s, t) = \int d\mathcal{O}\, e^{-s\mathcal{O}} P(C, \mathcal{O}, t). \tag{4}$$

The moment generating function $Z(s, t)$ is recovered from this Laplace transform as $Z(s, t) = \sum_C \hat{P}(C, s, t)$. The Laplace transform $\hat{P}(C, s, t)$ satisfies a modified Master equation for its time-evolution (see, *e.g.*, [16]),

$$\partial_t \hat{P} = \mathbb{W}_s \hat{P}, \tag{5}$$

where the modified Master operator $\mathbb{W}_s$ is defined as

$$(\mathbb{W}_s)_{C'C} = W_s(C \to C') - r_s(C)\delta_{CC'} \;+\; \delta r_s(C)\delta_{CC'}. \tag{6}$$

and where $\delta r_s(C) = r_s(C) - r(C) - sb(C)$. The main idea behind the cloning algorithm [7, 8] comes from interpreting this time-evolution equation as a modified dynamics with rates

$$W_s(C \to C') = e^{-sa(C,C')} W(C \to C') \tag{7}$$

and escape rate

$$r_s(C) = \sum_{C'} W_s(C \to C'). \tag{8}$$

By rewriting the modified Master equation (5) by using these definitions, we find that this Master equation can be interpreted as a combined process of this modified stochastic process (equation (7)) with a selection mechanism by rates

$$\delta r_s(C) = r_s(C) - r(C) - sb(C). \tag{9}$$

As we detail below, the CGF $\psi(s)$ is recovered from the exponential growth (or decay) rate of a population evolving according to these rules.

C. Continuous-Time Population Dynamics (Constant-Population Approach)

The basic idea of the population dynamics algorithm is as follows: We prepare N_c copies of the system and we evolve them according to the transition rates $W_s(C \to C')$ given by equation (7). During this evolution some copies are repeatedly multiplied or eliminated according to the selection mechanism whose rate is given by equation (9). This selection process can be performed in a number of ways. One of them consists in keeping the total number of clones constant for each pre-fixed time-interval Δt (see Ref. [7] and also the Part I [1]). Another one, (that we will use throughout this Part II) consists in performing these selection processes along with each evolution of the copies [6, 9, 10]. A detailed description of this last algorithm is presented below

The Cloning Algorithm

Lets consider N_c clones (or copies) of the system. We denote by $\mathbf{t} = \{t^{(i)}\}_{i=1,...,N_c}$ the evolution times and by $c = \{c_i\}_{i=1,...,N_c}$ the configurations of each clone. Their initial configurations do not affect the resulting scaled cumulant generating function in the large-time limit. However, for the concreteness of the discussion, without loss of generality, we assume that these copies have the same configuration C at $\mathbf{t} = 0$. The cloning algorithm is constituted of the repetition of the following procedures.

1. Find the clone whose evolution time is the smallest among all the clones: Find $j = \text{argmin}_i t^{(i)}$.
2. Choose a waiting time $\Delta t(c_j)$ for clone j from an exponential law of parameter $r_s(c_j)$. The change of configuration will occur at $t^{(j)} + \Delta t(c_j)$ (*i.e.*, clone j stays in the same state until time $t^{(j)} + \Delta t(c_j)$).
3. The state c_j is changed to c'_j with probability $W_s(c_j \to c'_j)/r_s(c_j)$.
4. Compute $y_j = \lfloor Y(c_j) + \epsilon \rfloor$, where the cloning factor $Y(c_j)$ is defined as $e^{\Delta t(c_j)\,\delta r_s(c_j)}$ and ϵ is a random number uniformly distributed on $[0, 1]$.
5. Eliminate or multiply clone c_j depending on y_j: If $y_j = 0$, we remove this copy from the ensemble, and if $y_j > 0$, we make $y_j - 1$ clones of this copy.
6. In order to keep the total number of copies constant, if $y_j = 0$, we choose randomly and uniformly a clone k, $k \neq j$ and copy it. If $y_j > 1$, we choose randomly and uniformly $y_j - 1$ clones from the ensemble and we erase them.

D. Cumulant Generating Function Estimator

The estimator $\Psi_s^{(N_c)}$ of the CGF can be obtained from the algorithm we just described from the exponential growth rate that the population would present if it was not kept constant [6]. More precisely, the estimator $\Psi_s^{(N_c)}$ is defined as

$$\Psi_s^{(N_c)} = \frac{1}{t} \log \prod_{i=1}^{\mathcal{K}} X_i, \tag{10}$$

where $X_i = (N_c + y_i - 1)/N_c$ are the "growth" factors at each step i of the procedure described above, and $\mathcal{K}$ is the total number of configuration changes in the full population up to time t (which has not to be confused with K). It is important to remark (as was discussed in [17] in a non-constant population context) that this growth rate can be also computed from a linear fit over the reconstructed log-population and the initial transient regime, where the discreteness effects are present, can be discarded in order to obtain a better estimation.

For a real implementation of the algorithm, we need to launch the simulation many times (where we denote by R the number of realizations of the same simulation). Then, the CGF estimator should be calculated as the arithmetic mean of the obtained estimator (equation (10)). As the simulation does not stop exactly at T (as discussed in Sec. 3.2 of [17]) but at some time $t_r^{\mathcal{F}} \leq T$ (which is different for every $r \in \{1, ..., R\}$), the average over R realizations of $\Psi_s^{(N_c)}$ is then correctly defined as

$$\overline{\Psi_s^{(N_c)}} = \frac{1}{R} \sum_{r=1}^{R} \frac{1}{t_r^{\mathcal{F}}} \log \prod_{i=1}^{\mathcal{K}_r} X_i^r. \tag{11}$$

However, we have observed that for not too short simulation times T, $\left| \overline{\Psi_s^{(N_c)}(T)} - \overline{\Psi_s^{(N_c)}(t_r^{\mathcal{F}})} \right|$ is small. By assuming $t_r^{\mathcal{F}} \approx T$, equation (11) is approximated as

$$\overline{\Psi_s^{(N_c)}} \simeq \frac{1}{R} \frac{1}{T} \sum_{r=1}^{R} \log \prod_{i=1}^{\mathcal{K}_r} X_i^r. \tag{12}$$

Equation (12) allows us to estimate the CGF using the constant-population approach of the continuous-time cloning algorithm for a s-biased Markov process, given a fixed number of clones N_c, a simulation time T and R realizations of the algorithm.

E. Example Model: A Two-State Annihilation-Creation Dynamics

Although the cloning algorithm explained above is general, and although we expect that the scaling method explained in the following sections can be applied to more general models, we focus our numerical study to a simple two-state annihilation-creation dynamics with transition rates

$$\begin{aligned} 0 &\xrightarrow{c} 1 \\ 1 &\xrightarrow{1-c} 0. \end{aligned} \tag{13}$$

We take the additive observable $\mathcal{O}$ as the activity K. In this system, it is possible to obtain the analytical expression for the cumulant generating function $\psi(s)$ as the largest eigenvalue of $\mathbb{W}_s$, which is

$$\psi(s) = -\frac{1}{2} + \frac{1}{2}\sqrt{1 - 4c(1-c)(1 - e^{-2s})}. \tag{14}$$

Equation (14) allows us to quantify the quality of the numerical results obtained from the algorithm described above.

III. THE LARGE DEVIATION FUNCTION FOR A FINITE DURATION OF TIME

In this section, we study the large-time behavior of the CGF estimator, at a fixed number of clones N_c, and we

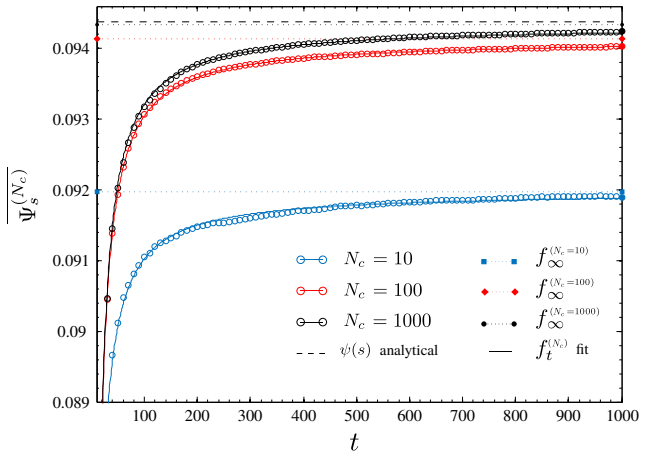

FIG. 1. Average over $R = 10^4$ realizations of the CGF estimator $\Psi_s^{(N_c)}$ (equation (12)) as a function of duration t of the observation window, for $N_c \in \{10, 100, 1000\}$ clones. The analytical expression for the large deviation function $\psi(s)$ (equation (14)) is shown with a black dashed line and the fitting function $f_t^{(N_c)}$ encoding the finite-t scaling (equation (16)) are shown with continuous curves. The (*a priori*) best estimation of the large deviation function would be given by $\overline{\Psi_s^{(N_c)}}$ at the largest simulation time $T = 1000$, which are shown with solid circles. The extracted infinite-time behavior $f_\infty^{(N_c)}$ are shown as dotted lines and circles ($N_c = 10$), diamonds ($N_c = 100$) and squares ($N_c = 1000$). The parameters of the model are $c = 0.3$, $s = -0.2$.

discuss how to use the scaling form of this behavior in order to extract the asymptotic value of the estimator at infinite time. Fig. 1 presents the average over $R = 10^4$ realizations of the estimator of the CGF $\overline{\Psi_s^{(N_c)}}$ as a function of the (simulation) time for given numbers of clones $N_c = \{10, 100, 1000\}$. It is compared with the analytical value $\psi(s)$ (black dashed line). The curve $\overline{\Psi_s^{(N_c)}}$ shows the estimation of the CGF that we would have obtained if we had considered a simulation time t smaller than the maximal simulation time T (which in this case is equal to $T = 1000$). As can be seen in Fig. 1 for a small number of clones ($N_c = 10$) and even if we would consider an "infinite" simulation time, the best estimation obtained from the continuous-time cloning algorithm is highly deviated from the analytical value $\psi(s)$. But as expected, as N_c and the simulation time t become larger, the obtained CGF estimator gets closer to the analytical value $\psi(s)$.

One can expect that $\psi(s)$ will be obtained from the estimator in the $T \to \infty$ limit and $N_c \to \infty$ limit:

$$\lim_{N_c\to\infty} \lim_{T\to\infty} \overline{\Psi_s^{(N_c)}}(T) = \psi(s). \tag{15}$$

Indeed, this was explicitly derived in Part I of this paper from a different version of the cloning algorithm (See [1] for the detail) under general hypotheses. In the implementation of the algorithm, this infinite-time and -size limit is in practice achieved by considering a large enough simulation time T and a large enough number of clones N_c. In other words, the best naive estimation of the large deviation function that we can obtain from the continuous-time cloning algorithm would be given by the value of $\overline{\Psi_s^{(N_c)}}$ at largest simulation time T with the largest number of clones N_c, *i.e.*, the value of $\overline{\Psi_s^{(N_c)}}(T)$ which is shown as a black solid circle in Fig. 1 for $T = 1000$ and $N_c = 1000$. The expression "large enough" is of course vague but motivates our analysis of the actual dependence of the estimator with T and N_c. In this section, we especially focus on the dependence with respect to T.

A. t^{-1} Scaling

We define a fitting curve $f_t^{(N_c)}$ as

$$f_t^{(N_c)} \equiv f_\infty^{(N_c)} + b_t^{(N_c)} t^{-1}, \tag{16}$$

where $f_\infty^{(N_c)}$ and $b_t^{(N_c)}$ are fitting parameters. We determine these parameters from the least squares method by minimizing the deviation from $\overline{\Psi_s^{(N_c)}}(t)$. The obtained results are shown with continuous curves in Fig. 1. One important feature about these fits $f_t^{(N_c)}$ are their t^{-1} scaling: the fitting curves describe well $\overline{\Psi_s^{(N_c)}}(t)$, which implies that $\overline{\Psi_s^{(N_c)}}(t)$ converges to its infinite value proportionally to $1/t$. This property can be derived from the remark that the cloning algorithm itself is described by a Markov process: By expressing the number of clones by a birth-death process, we may construct a meta-Markov process that describes the cloning algorithm. Once this is constructed, the CGF estimator (10) is regarded as the time-average of the observable X_i for such meta-Markov process. We now recall that, in general, time-averaged quantities converge to their infinite-time limit with an error proportional to $1/t$, when the distribution function of the variable converges exponentially (as in our Markov processes). We thus find that the scaling property (16) is satisfied. For more details of how to construct this meta-dynamics, see Part I [1] where we indeed explicitly devise its generator for a discrete-time version of the cloning algorithm.

We note that $f_\infty^{(N_c)}$ is expected to converge to $\psi(s)$ as $N_c \to \infty$, see equation (15). For checking this property, we define the distance D between $\psi(s)$ and its numerical estimator $\overline{\Psi_s^{(N_c)}}$,

$$D\big(\overline{\Psi_s^{(N_c)}}, \psi(s)\big) = \big|\overline{\Psi_s^{(N_c)}} - \psi(s)\big|. \tag{17}$$

This quantity is shown in Fig. 2 as a function of t in log-log scale. As we can see, as N_c increases, $\log D$ behaves as straight line with slope -1 on a time window which grows with N_c. This means that when $N_c \to \infty$, the

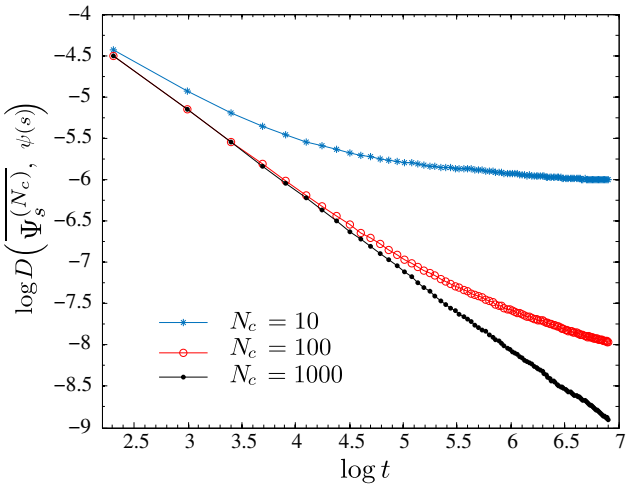

FIG. 2. Distance D between the analytical value of the CGF $\psi(s)$ and its numerical estimator $\overline{\Psi_s^{(N_c)}}$, as a function of time t in log-log scale (equation (17)). This distance behaves as a power law of exponent -1 on a time window which increases as N_c increases. This illustrates the limit (15).

following scaling is satisfied

$$\left|\overline{\Psi_s^{(N_c)}} - \psi(s)\right| \sim t^{-1}. \tag{18}$$

This illustrates that $f_\infty^{(N_c)}$ converges to $\psi(s)$ as $N_c \to \infty$.

B. Infinite-Time Limit of the CGF Estimator

1. *Extraction from Finite-Time Simulations*

Equation (16) allows us to extract the infinite-time limit of the CGF using the continuous-time cloning algorithm. Once we obtain the fitting curve $f_t^{(N_c)}$ that describes correctly the time-dependence of $\overline{\Psi_s^{(N_c)}(t)}$, we can use the fitting parameter $f_\infty^{(N_c)}$ to estimate the infinite-time limit of $\overline{\Psi_s^{(N_c)}(t)}$, *i.e.*,

$$\lim_{t\to\infty} \overline{\Psi_s^{(N_c)}(t)} = f_\infty^{(N_c)}. \tag{19}$$

We denoted this infinite-time limit as $f_\infty^{(N_c)}$ and it is shown with dotted lines and circles ($N_c = 10$), diamonds ($N_c = 100$) and squares ($N_c = 1000$) in Fig. 1. This asymptotic limit to which $\Psi_t^{(N_c)}$ tends as $t \to \infty$ provides a better numerical estimate of $\psi(s)$ than $\overline{\Psi_s^{(N_c)}(T)}$ (which is obtained from finite simulation time) and it can be achieved even for shorter simulation times through a fit of the form given in equation (16) on the numerical estimator $\overline{\Psi_s^{(N_c)}(t)}$ (See Sec. V for the summary of this extraction method).

2. *Scaling Limit*

Although the method to extract the infinite-time limit based on fitting (described above) is straightforward and it has been verified to yield good results, an alternative method to estimate $f_\infty^{(N_c)}$ is presented here. If we modify $\psi(s)$ by adding some values δ properly chosen, $D\big(\overline{\Psi_s^{(N_c)}}, \psi(s)+\delta\big)$ presents a t^{-1} behavior, where the window of this scaling depends on the value of δ. We expect that the δ maximizing the duration of this window corresponds to $f_\infty^{(N_c)} - \psi(s)$.

The problem of determining such a δ thus reduces to finding a value of Ψ_∞ around $\psi(s)$, such that $D\big(\overline{\Psi_s^{(N_c)}}, \Psi_\infty\big)$ is linear in time in log-log scale on a maximally extended window of time. In other words, we have to determine the best Ψ_∞ such that

$$\left|\overline{\Psi_s^{(N_c)}} - \Psi_\infty\right| \sim t^{-1}. \tag{20}$$

This can be done (of course) without knowing the analytical value of the large deviation function and should be right even for small N_c. A possible method in order to determine Ψ_∞ is described below.

Let $\big[\psi(s)-\delta_1, \psi(s)+\delta_2\big]$ be an interval (non necessarily symmetrical) around $\psi(s)$ (which is not necessarily to be known). We define the quality $Q(\Psi)$ as

$$Q(\Psi) = \Big\langle \Big| \log D\big(\overline{\Psi_s^{(N_c)}}, \Psi\big) - F_\Psi^{(N_c)} \Big| \Big\rangle, \tag{21}$$

where $F_\Psi^{(N_c)} = F\big(D\big(\overline{\Psi_s^{(N_c)}}, \Psi\big)\big)$ is an affine fit of $D\big(\overline{\Psi_s^{(N_c)}}, \Psi\big)$ in time, in log-log scale. The value of $\Psi_\infty \in \big[\psi(s)-\delta_1, \psi(s)+\delta_2\big]$ is determined as the one minimizing this $Q(\Psi_\infty)$. We indeed checked that $f_\infty^{(N_c)}$ and Ψ_∞ coincide within numerical uncertainties.

C. Distribution of $\Psi_s^{(N_c)}$

From relation (12), one can infer that the dispersion of the distribution of $\Psi_s^{(N_c)}$ depends on the simulation time t. This determines whether or not a large number of realizations R is required in order to minimize the statistical error. In fact, as seen in Fig. 3, the dispersion of $\Psi_s^{(N_c)}$ is wider for shorter simulation times. This distribution is concentrated around its mean value that is displaced towards the analytical value $\psi(s)$, as the simulation time and the number of clones increase. We numerically confirm that these distributions are well-approximated by a Gaussian distribution

$$P\left(\Psi_s^{(N_c)}\right) \sim A e^{-\frac{1}{C^2}\left(\Psi_s^{(N_c)} - B\right)^2}, \tag{22}$$

where B is $\overline{\Psi_s^{(N_c)}}$ and A and C are numerical parameters. As seen in Fig. 4, these parameters A and $1/C^2$ are of

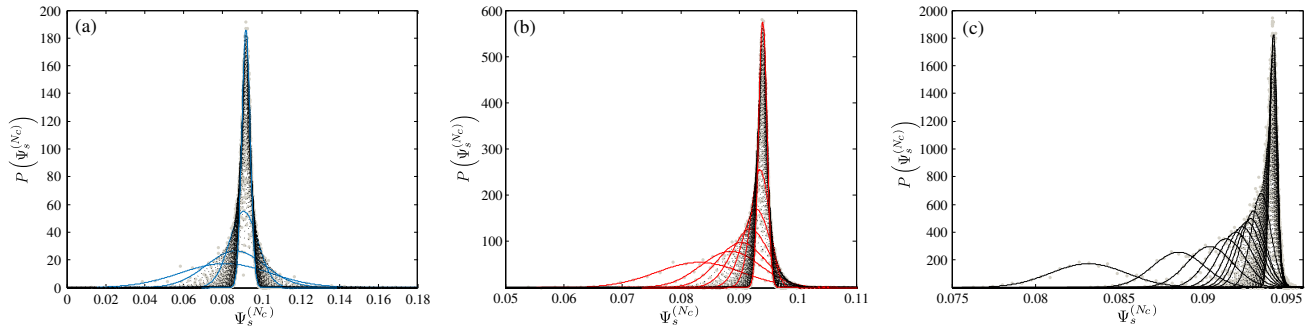

FIG. 3. Distribution $P\left(\Psi_s^{(N_c)}\right)$ of the large deviation function estimator $\Psi_s^{(N_c)}$ for **(a)** $N_c = 10$, **(b)** $N_c = 100$ and **(c)** $N_c = 1000$ and simulation times $t \in [10, 1000]$. Each realization ($R = 10^4$ for each simulation time) is shown with gray dots meanwhile its respective Gaussian fit (equation (22)) is shown with a dotted or a continuous curve. The dispersion of $\Psi_s^{(N_c)}$ is wider for shorter simulation times and small N_c. The mean value of the distribution displaces towards the theoretical value as the simulation time and the number of clones increases.

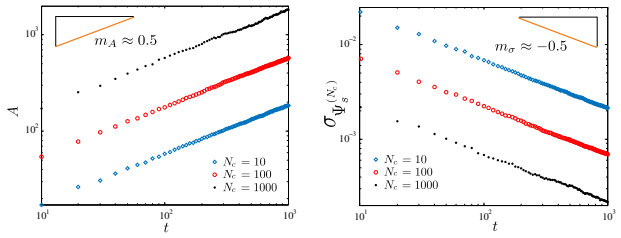

FIG. 4. Time evolution of the parameters A and C determined numerically from a Gaussian fit (equation (22)) of the distribution of large deviation functions $\Psi_s^{(N_c)}$ (Fig. 3). The parameters A and C were found to behave in time as $A = \mathcal{O}(t^{1/2})$ (left) and $1/C^2 = \mathcal{O}(t)$. Due to the relation between C and the standard deviation $\sigma_{\Psi_s^{(N_c)}}$, $\sigma_{\Psi_s^{(N_c)}}$ also behaves as $\sigma_{\Psi_s^{(N_c)}} = \mathcal{O}(t^{-1/2})$ which is presented on the right. The values $m_A \approx 0.5$ and $m_\sigma \approx -0.5$ are the slopes of A and $\sigma_{\Psi_s^{(N_c)}}$, in log-log scale.

the order of $t^{1/2}$ and t. We note that, from this scaling, the variance $\sigma_{\Psi_s^{(N_c)}}$ is also of the order of $t^{-1/2}$.

A mathematical argument to explain this obtained Gaussian distribution is given as follows. If at any given time (not necessarily at T), we take the following rescaling

$$\hat{\Psi}_s^{(N_c)} = \frac{\Psi_s^{(N_c)} - \overline{\Psi_s^{(N_c)}}}{\sigma_{\Psi_s^{(N_c)}}}, \tag{23}$$

where

$$\sigma^2_{\hat{\Psi}_s^{(N_c)}} = \frac{1}{R-1}\sum_{r=1}^{R}\left|\left(\Psi_s^{(N_c)}\right)_r - \overline{\Psi_s^{(N_c)}}\right|^2 \tag{24}$$

is the variance of the R realizations of $\Psi_s^{(N_c)}$ and $\left(\Psi_s^{(N_c)}\right)_r$ is $\Psi_s^{(N_c)}$ in the realization r, then this rescaled CGF $\hat{\Psi}_s^{(N_c)}$ follows a standard normal distribution (according to the central limit theorem):

$$P\left(\hat{\Psi}_s^{(N_c)}\right) = \frac{1}{\sqrt{2\pi}} e^{-\frac{1}{2}\left(\hat{\Psi}_s^{(N_c)}\right)^2}, \tag{25}$$

where $\sigma^2_{\hat{\Psi}_s^{(N_c)}} \approx 1$. This rescaling produces a collapse of the distributions $P\left(\hat{\Psi}_s^{(N_c)}\right)$ for $\forall t$ and $\forall N_c$ (Fig. 5).

In other words, by considering the scaling given by the definition (23) we focus only on the small fluctuation of $\Psi_s^{(N_c)}$ around $\overline{\Psi_s^{(N_c)}}$, which can be described by a Gaussian distribution. But in general, the distribution function is not necessarily described by this form, and we need to consider a large deviation principle as it is explained below.

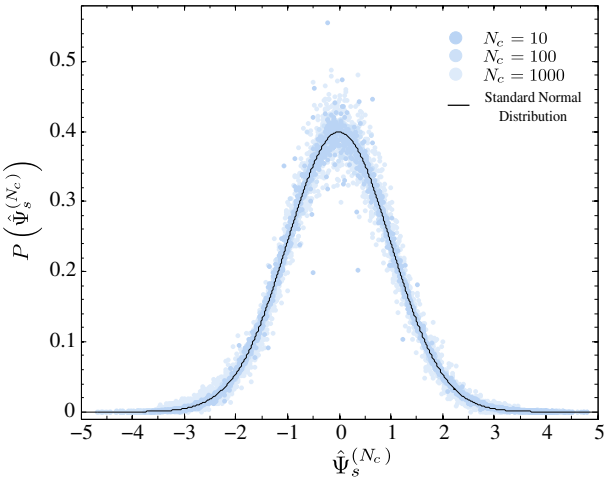

FIG. 5. The distribution function of the rescaled variable $\hat{\Psi}_s^{(N_c)}$ (23). Compatible with the central limit theorem (equation (25)), a collapse of the distribution function into a standard normal distribution for different number of clones is observed.

Since $\Psi_s^{(N_c)}$ is itself an additive observable of the dynamics of the ensemble of clones (see Part I, Sec. III for more details), the distribution of the CGF estimator $\Psi_s^{(N_c)}$ satisfies itself a large deviation principle of the form

$$P\big(\Psi_s^{(N_c)}\big) \sim e^{-tI_{N_c}\left(\Psi_s^{(N_c)}\right)}, \tag{26}$$

where $I_{N_c}\big(\Psi_s^{(N_c)}\big)$ is the rate function (LDF). Here, we study if this large deviation function can be numerically evaluated from the empirical distribution $P\big(\Psi_s^{(N_c)}\big)$ as

$$I_{N_c}\big(\Psi_s^{(N_c)}\big) \approx -\frac{1}{t}\log P\big(\Psi_s^{(N_c)}\big) \tag{27}$$

for a large t. [1]

The numerical estimation of the right-hand side of the last expression at final simulation time T is shown in Fig. 6, where we have defined

$$\hat{I}_{N_c}\big(\Psi_s^{(N_c)}\big) \equiv -\frac{1}{t}\log P\big(\Psi_s^{(N_c)}\big) + \frac{1}{t}\log P\big(\overline{\Psi_s^{(N_c)}}\big) \tag{28}$$

so that $\hat{I}_{N_c}\big(\overline{\Psi_s^{(N_c)}}\big) = 0$. In the same figure, we also show $\overline{\Psi_s^{(N_c)}(T)}$ as vertical dotted lines which correspond to the minima of the rate function $\hat{I}_{N_c}\big(\Psi_s^{(N_c)}\big)$. As can be seen, these minima are displaced towards the analytical value $\psi(s)$ (shown with a dashed line) as $t \to \infty$. The rate function $\hat{I}_{N_c}$ also becomes more concentrated as N_c increases.

As we already know from section III C, the obtained rate function is well-approximated by a quadratic form (because the logarithm of the distribution function is proportional to the rate function). However, as shown in Sec. IV of Part I, these LDFs are not quadratic in general, which indicates that the full shape of the large deviation function could not be obtained from our simulations. These rare events are indeed not relevant for our simple model, but we expect that they might play an important role in more complicated systems, such as the ones presenting dynamical phase transitions.

IV. THE LARGE DEVIATION FUNCTION FOR A FINITE NUMBER OF COPIES

In this section, for a fixed duration T of the observation window, we study the behavior of the CGF estimator as a function of the population size N_c (see also Sec. III C of Part I [1] for an analytical study to this problem).

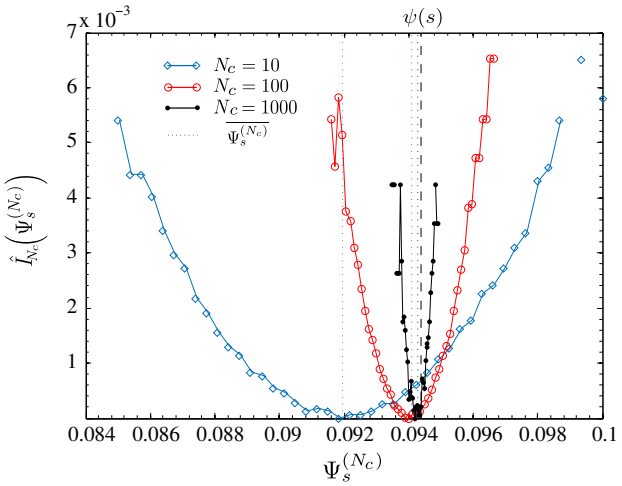

FIG. 6. Rescaled rate function $\hat{I}_{N_c}\big(\Psi_s^{(N_c)}\big)$ (equation (28)) of the large deviation principle (equation (26)). Numerical evaluations were made for three fixed population sizes $N_c \in \{10, 100, 1000\}$. The average over R realizations of the CGF estimator $\overline{\Psi_s^{(N_c)}(T)}$ corresponds to the minimum of $\hat{I}_{N_c}\big(\Psi_s^{(N_c)}\big)$ (dotted lines). The most probable value of the rate function (vertical dashed lines) moves to the analytical value $\psi(s)$ as $t \to \infty$ and presents a smaller width as N_c increases.

In Fig. 7, we present the behavior of the CGF estimator $\overline{\Psi_s^{(N_c)}(T)}$ as we increase the number of clones, for a given fixed (simulation) time T. We considered four values of final simulation times $T = \{200, 300, 500, 1000\}$ and population sizes in the range $10 \leq N_c \leq 1000$. As already mentioned, the value $\big\langle \Psi_s^{(N_c)}(T) \big\rangle$ is generally considered as the best estimation of the large deviation function we can obtain for a given simulation time T and a given number of clones N_c using the continuous-time cloning algorithm. However in Sec. III B 1 we saw how the estimation of $\psi(s)$ can be improved by extracting the infinite-time limit $f_\infty^{(N_c)}$ from the finite-t scaling (equation (16)). Below, we explain how to perform a similar extraction with respect to the number of clones: *i.e.*, how to estimate the infinite-N_c limit from a set of finite-N_c simulations.

A. N_c^{-1} Scaling

We define a fitting curve as

$$g_{N_c}^{(T)} = g_\infty^{(T)} + \tilde{b}_{N_c}^{(T)} N_c^{-1}, \tag{29}$$

where $g_\infty^{(T)}$ and $\tilde{b}_{N_c}^{(T)}$ are fitting parameters. The obtained $g_{N_c}^{(T)}$ fitted to $\overline{\Psi_s^{(N_c)}(T)}$ (as a function of N_c) is shown in Fig. 7 with continuous curves. As can be seen, the fitting

[1] Strictly speaking

$$I_{N_c}\big(\Psi_s^{(N_c)}\big) = \lim_{t\to\infty} -\frac{1}{t}\log P\big(\Psi_s^{(N_c)}\big)$$

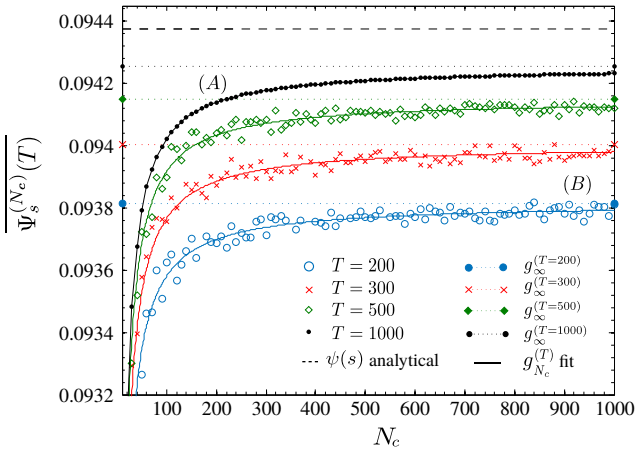

FIG. 7. Estimator $\overline{\Psi_s^{(N_c)}(T)}$ (equation (12)) of the CGF for given (final simulation) times $T = \{200, 300, 500, 1000\}$ as a function of the number of clones N_c (on the range $10 \leq N_c \leq 1000$). The analytical value $\psi(s)$ (equation (14)) is shown with a dashed line and the fits $g_{N_c}^{(T)}$ (equation (29)) with continuous curves. A large simulation time for a small number of clones, shown in (A), produces a better estimation compared to the one given by the largest number of clones with a relatively short simulation time, which is shown in (B). The best CGF estimation we can naively obtain would be given by $\overline{\Psi_s^{(N_c)}(T)}$ at largest simulation time T and largest number of clones N_c. However, the extracted infinite-size limits $g_\infty^{(T)}$ provide a better estimation in comparison. These limits are shown with dotted lines and circles ($T = 200$), crosses ($T = 300$), diamonds ($T = 500$) and dots ($T = 1000$). Additionally, $c = 0.3$ and $s = -0.2$.

curves describe well the dependence in N_c of $\overline{\Psi_s^{(N_c)}(T)}$, which means that $\overline{\Psi_s^{(N_c)}(T)}$ converges to its infinite N_c limit with an error proportional to $1/N_c$. This scaling was proved under general assumptions in Sec. III C of Part I [1]. However, it is important to remark that this numerical observation is interesting because the proof in Part I does not cover (i) the continuous-time algorithm used in this Part II and (ii) the CGF estimator $\overline{\Psi_s^{(N_c)}(T)}$ at finite T (in the proof was considered the $T \to \infty$ limit). The generalization of the argument presented in Part I in order to cover these cases (i) and (ii) is an open direction of research.

B. Infinite-Size Limit of the CGF Estimator: Extraction from Finite-N_c Estimations

When the fitting $g_{N_c}^{(T)}$ describes well the N_c-dependence of $\overline{\Psi_s^{(N_c)}(T)}$, equation (29) allow us to the extract the $N_c \to \infty$ limit of $\overline{\Psi_s^{(N_c)}(T)}$ as:

$$\lim_{N_c \to \infty} \overline{\Psi_s^{(N_c)}(T)} = g_\infty^{(T)}. \tag{30}$$

This infinite-size limit $g_\infty^{(T)}$ is shown in Fig. 7 as dotted lines. As can be seen, $g_\infty^{(T)}$ is closer to $\psi(s)$ than $\overline{\Psi_s^{(N_c)}(T)}$ at the largest N_c. It is important to remark that this extraction of $\lim_{N_c \to \infty} \overline{\Psi_s^{(N_c)}(T)}$ can be achieved even for smaller numbers of clones.

We combine the finite-time and finite-size scalings of the CGF estimator in Sec. V when we present a method which allows us to extract the infinite-time infinite-size limit from simulations performed with a small number of clones and with a small (simulation) time.

C. Distribution of $\Psi_s^{(N_c)}(T)$ and its Large Deviations

From the results presented in Sec. III C, for the range of realization $R \sim 10^4$ that we considered, one can find that at final simulation time T and for a given number of clones N_c, the distribution of $\Psi_s^{(N_c)}(T)$ is well approximated by the Gaussian distribution (22), where the parameter B is equal to $\left\langle \Psi_s^{(N_c)}(T) \right\rangle$ and with numerical parameters A and $1/C^2$ that are respectively of the order of $N_c^{1/2}$ and N_c (*i.e.* $\sigma_{\Psi_s^{(N_c)}(T)} = \mathcal{O}(N_c^{-1/2})$). A rescaling similar to the one given in equation (23) produces a collapse of the distribution of large deviations at final time into the standard normal distribution (25) for several values of N_c and R that we considered.

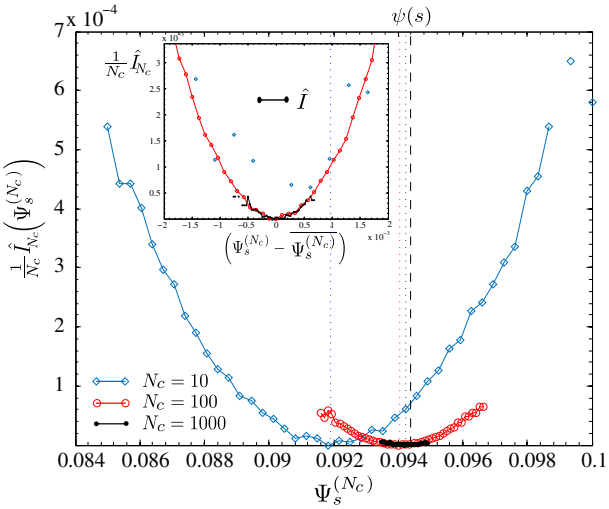

FIG. 8. Rescaled rate function $\frac{1}{N_c}\hat{I}_{N_c}\left(\Psi_s^{(N_c)}\right)$ and the same quantity as a function of $\check{\Psi}_s^{(N_c)} = \left(\Psi_s^{(N_c)} - \overline{\Psi_s^{(N_c)}}\right)$ (inset).

Fig. 8 shows the rescaled rate function $(1/N_c)\hat{I}_{N_c}\left(\Psi_s^{(N_c)}\right)$ (equation (28)) whose minimum converges to the analytical value $\psi(s)$ (black dashed line) as $N_c \to \infty$. In the infinite-time infinite-size limit of $\Psi_s^{(N_c)}$, it is thus compatible with a large deviation

principle of rate function given by

$$I\left(\Psi_s^{(N_c)}\right) = -\lim_{N_c\to\infty}\frac{1}{N_c}\lim_{t\to\infty}\frac{1}{t}\log P\left(\Psi_s^{(N_c)}\right) \qquad (31)$$

which is shown (rescaled) with black dots in Fig. 8 (See Sec. III of Part I for the argument which justifies this large deviation principle). Moreover, by performing the shift $\check{\Psi}_s^{(N_c)} = \left(\Psi_s^{(N_c)} - \overline{\Psi_s^{(N_c)}}\right)$ we can see in the inset of Fig. 8 the superposition of quadratic deviations of the numerical estimator $\Psi_s^{(N_c)}$ around the minimum of the rate function $\hat{I}$ (especially for $N_c = 100, 1000$).

V. THE LARGE DEVIATION FUNCTION IN THE INFINITE-TIME - INFINITE-SIZE LIMIT

We have shown in Sec. III B 1 that for any fixed population N_c, it is possible to extract the infinite-time limit $f_\infty^{(N_c)}$ (equation (16)) from a finite-time CGF estimation. Similarly in Sec. IV B, we have shown, for a given final (simulation) time T, how one can extract the infinite-size limit $g_\infty^{(T)}$ (equation (29)) from finite-N_c CGF estimations. Moreover, if we consider a set of simulations performed at population sizes $\vec{N_c} = \{N_c^{(1)}, ..., N_c^{(j)}\}$, one observes that $f_\infty^{N_c}$ behaves as a function of N_c (see Fig. 10(a)) as

$$f_\infty^{(N_c)} = f_\infty^\infty + b_\infty^{(N_c)} N_c^{-1} \qquad (32)$$

exhibiting itself $1/N_c$ corrections for large but finite N_c (see also Part I). These numerical results illustrate that the analytical results, found for the cloning algorithm in discrete-time representation in Part I, are also valid in its continuous-time version (that we have used in the present Part II). The observed scalings provide a method to extract the infinite-time infinite-size limit of the CGF estimator $\Psi_s^{N_c}$, obtained from the simple scalings of the finite-time and finite-size corrections. As we present below, this scaling yields the better estimation of the large deviation function within the cloning algorithm, and importantly, it can be used for a relatively short simulation time with a relatively small number of clones at least in our numerical example.

A. Infinite-Time and -Size Limit from the Finite-Time and -Size Scalings of the CGF Estimator: An Example

On Fig. 9, we present a complete picture of the behavior of the estimator $\overline{\Psi_s^{(N_c)}}(t)$ as a function of the duration t and of the number of clones N_c. The surface shown in Fig. 9 shows $\overline{\Psi_s^{(N_c)}}(t)$ for a maximum simulation time $T = 500$ and a maximum number of clones $\max \vec{N_c} = 100$. The estimation was evaluated using the continuous-time cloning algorithm (as described in Sec. II C and II D and as shown on Fig. 1) for 10 values of N_c from $\vec{N_c} = \{10 \times i\}_{i=1,2,...,10}$. The value of the estimator at the final simulation time T is represented with black circles (*c.f.*, Fig. 7). The analytical expression for the large deviation function $\psi(s)$ (equation (14)) is shown in a black dashed line.

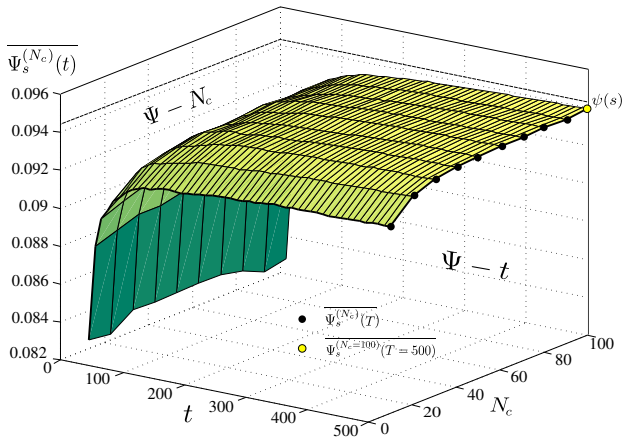

FIG. 9. Estimator of the large deviation function $\overline{\Psi_s^{(N_c)}}(t)$ as a function of time and the number of clones. The estimator $\overline{\Psi_s^{(N_c)}}(T)$ at final simulation time $T = 500$ as a function of the number of clones (up to $N_c = 100$) is shown as black circles ($\overline{\Psi_s^{(N_c=100)}}(T = 500)$ is shown as a yellow circle). The analytical expression (14) for the large deviation function $\psi(s)$ is shown as a black dashed line. Additionally, $s = -0.2$, $c = 0.3$, and $R = 10^3$.

When using the cloning algorithm, the numerical estimation of the CGF is normally taken as $\overline{\Psi_s^{(N_c)}}(t)$ for the largest simulation time $t = T$ and the largest number of clones [9, 10], which in this case corresponds to $\overline{\Psi_s^{(N_c=100)}}(T = 500)$ which is shown in Fig. 9 with a yellow circle.

Using the results from sections III A, III B 1, IV A, IV B, and V we detail below a method which allows us to extract the infinite-time infinite-size limit from finite (and short) simulation times and finite (and small) number of clones. We emphasize that for this example we consider just a half of the simulation time that we used in Fig. 1, and 1/10 of the number of clones we considered in Fig. 7.

We show on Fig. 10(a) the projection of the surface of Fig. 9 on the plane $\Psi - t$. The behavior in t of the estimator $\overline{\Psi_s^{(N_c)}}(t)$ is shown for $N_c = 10$ and $N_c = 100$, in blue dots in Fig. 10(a). The (standard) estimators of the CGF, $\overline{\Psi_s^{(N_c)}}(T)$ (at the largest simulation time $t = T$), are shown in large blue dots in Fig. 10(a) (on the axis for $T = 500$) and (b) for all the values of N_c we are considering. These fitting curves $f_t^{(N_c)}$ (equation (16)) of the estimator are shown in black continuous lines (for $N_c = 10$ and $N_c = 100$) and black dotted lines (for other intermediate values of N_c). Next, we show in Fig. 10(b)

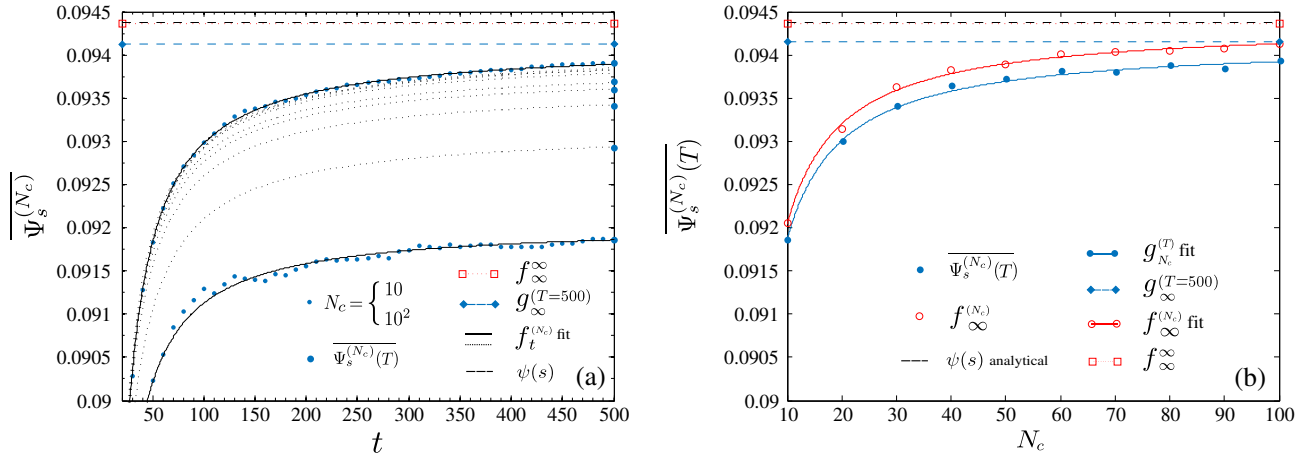

FIG. 10. **(a)** Projection of the surface represented in Fig. 9 over the plane $\Psi - t$. $\overline{\Psi_s^{(N_c)}}(t)$ is represented for $N_c = 10$ and $N_c = 100$ with blue dots. The estimations $\overline{\Psi_s^{(N_c)}}(T)$ of the large deviation (at the final simulation time $T = 500$) are shown in large blue dots for all the values of N_c considered. The fit in time (equation (16)) over $\overline{\Psi_s^{(N_c)}}(t)$ is shown as black solid lines (for $N_c = 10$ and $N_c = 100$) and dotted lines (for other values of N_c). **(b)** Projection at the final simulation time $T = 500$ on the plane $\Psi - N_c$, $\overline{\Psi_s^{(N_c)}}(T)$ is shown in large blue dots. The infinite-time limit $f_\infty^{(N_c)}$ as a function of N_c (see equation (16)) is represented in red circles. The results of fitting $\overline{\Psi_s^{(N_c)}}(T)$ (equation (29)) and $f_\infty^{(N_c)}$ (equation (32)) are shown with blue and red solid curves respectively. The infinite-N_c limit $g_\infty^{(T)}$ is shown with blue dashed line and diamonds meanwhile the infinite-size and time limit f_∞^∞ is shown with a red dotted line in both of **(a)** and **(b)**. The extracted limit f_∞^∞ agrees remarkably well with the analytical value of the large deviation function $\psi(s)$ (equation (14)), shown in black dashed line.

the projection of the surface of Fig. 9 on the plane $\Psi - N_c$ where the time has been set to the largest $t = T$. The fitting curve $g_{N_c}^{(T)}$ (equation (29)) on $\overline{\Psi_s^{(N_c)}}(T)$ is shown as a blue solid line in Fig. 10(b). As we discussed in Sec. IV A, from these curves, we can extract the infinite-size limit of the CGF estimator $g_\infty^{(T)}$, which is shown as a blue dashed line and diamonds. Finally, the infinite-time limit $f_\infty^{(N_c)}$ extracted from the fitting on $\overline{\Psi_s^{(N_c)}}(t)$ for each value of N_c is shown as red circles in Fig. 10(b). According to equation (32), these values themselves are scaled as $1/N_c$ and their fits are shown as a red solid curve in the same figure. The scaling parameter f_∞^∞ obtained from this last step renders the infinite-size and the infinite-time limit of the CGF estimator (red dotted line and squares). This asymptotic estimator provides a better estimation of the large deviation function than $\overline{\Psi_s^{(N_c=100)}}(T = 500)$ (and also than $g_\infty^{(T)}$), as can be seen in Fig. 10. Below we summarize the method to extract this infinite-time - infinite-size limit.

B. The Scaling Method

The scaling method which allows us to extract the infinite-time and infinite-size limit of the CGF estimator is summarized as follows:

1. Determine the average over R realizations $\overline{\Psi_s^{(N_c)}}(t)$ (equation (12)) up to a final simulation time T for $\vec{N_c} = \{N_c^{(1)}, ..., N_c^{(j)}\}$.
2. Extract the infinite-time limit $f_\infty^{(N_c)}$ (equation (19)) from a fit in time $f_t^{(N_c)} = f_\infty^{(N_c)} + b_t^{(N_c)} t^{-1}$ (equation (16)) over $\overline{\Psi_s^{(N_c)}}(t)$ for each $N_c \in \vec{N_c}$.
3. Extract the infinite-size limit f_∞^∞ from a fit $f_\infty^{(N_c)} = f_\infty^\infty + b_\infty^{(N_c)} N_c^{-1}$ (equation (32)) in size of the infinite-time limit $f_\infty^{(N_c)}$.

The value f_∞^∞ represents the asymptotic limit to which the CGF estimator converges as the simulation time t and the number of clones N_c go to infinite, *i.e.*,

$$f_\infty^\infty = \lim_{N_c \to \infty} \lim_{t \to \infty} \overline{\Psi_s^{(N_c)}}(t). \tag{33}$$

The value obtained numerically is in very good agreement with the analytical one.

VI. A DIFFERENT CGF ESTIMATOR

Here we introduce another CGF estimator

$$\Phi_s^{(N_c)} = \frac{1}{T} \log \overline{\prod_{i=1}^{K_r} X_i^r} \tag{34}$$

which is different from $\overline{\Psi_s^{(N_c)}}$ defined in equation (12). We note that, in this definition, the average with respect

to realizations are taken *inside* the logarithm. As we discussed in Sec. IV.C of Part I, this estimator also provides a correct value of CGF $\psi(s)$ in the infinite-time infinite-N_c limits. This is thanks to the fact that the distribution of $\Psi_s^{(N_c)}$ concentrates around $\psi(s)$ in those limits (the so-called "self-averaging" property). At any finite population, one can rewrite $\Phi_s^{(N_c)}$ using the large-time LDF principle (26) as follows:

$$\Phi_s^{(N_c)} = \frac{1}{T} \log \overline{e^{T\Psi_s^{(N_c)}}} \tag{35}$$

$$= \frac{1}{T} \log \int d\Psi \; e^{-T\left[I_{N_c}(\Psi)+\Psi\right]} \tag{36}$$

which proves that in the large-T limit,

$$\Phi_s^{(N_c)} = \min_{\Psi} \left[I_{N_c}(\Psi) + \Psi \right], \tag{37}$$

to be compared to

$$\overline{\Psi_s^{(N_c)}} = \operatorname*{argmin}_{\Psi} I_{N_c}(\Psi). \tag{38}$$

Physically, the definition (34) amounts to estimate ψ from the exponential growth rate of the average of the final-T population of many small "islands" where the cloning algorithm would be operated, while the estimator (12) amounts to estimate ψ from growth rate of a large "island". The later is thus expected to be a better estimator of $\psi(s)$ than the former, *i.e.*, the estimator $\Phi_s^{(N_c)}$ thus appears *a priori* to be worse estimator than $\overline{\Psi_s^{(N_c)}}$ of $\psi(s)$. However, as shown in Sec. IV.C of Part I, at small $|s|$ and finite-N_c, a supplementary bias introduced by taking (34) instead of (12) in fact *compensates* the finite-N_c systematic error presented by (12), for the model that we consider. Namely, the error is $O(sN_c^{-1})$ for (12) while it is $O(s^2N_c^{-1})$ for (34). This fact is illustrated on Fig. 11, where we show that at small $s = 0.2$, $\Phi_s^{(N_c)}$ provides a better estimation of $\psi(s)$ than $\overline{\Psi_s^{(N_c)}}$, while at larger $|s|$ (here, $s = -1$) the two estimators yield a comparable error.

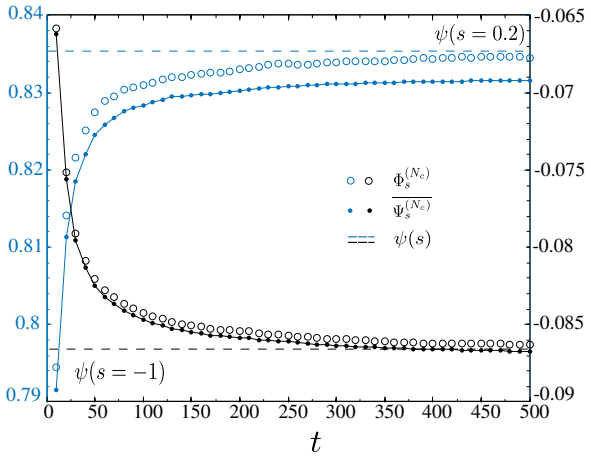

FIG. 11. Comparison between two different estimators of the large deviation function, $\overline{\Psi_s^{(N_c)}}$ (equation (12)) shown in dots and $\Phi_s^{(N_c)}$ (equation (34)) in circles. The analytical value $\psi(s)$ (equation (14)) is shown with a dashed line. Here we have also compared two different values of parameter $s = 0.2$ (blue) and $s = -1$ (black). Additionally, $N_c = 100$, $c = 0.4$, $T = 500$ and $R = 500$. As discussed in the text, the non-standard estimator $\Phi_s^{(N_c)}$ provides a better numerical evaluation of the CGF at small s.

VII. CONCLUSION

Direct sampling of the distribution of rare trajectories is a rather difficult numerical issue (see for instance [18] for an exhaustive study) because of the scarcity of the non-typical trajectories. We have shown how to increase the efficiency of a commonly used numerical method (the so-called cloning algorithm) in order to improve the evaluation of large deviation functions which quantify the distribution of such rare trajectories, in the long time limit. Following our analytical study (Part I, [1]), we have verified and exploited the finite-size and finite-time scaling behavior of estimators (and their distribution) in order to design an improved version of the algorithm which provides more reliable results (*i.e.* less affected by systematic errors due to finite time and finite population size).

We note that the scalings which rule the convergence to the infinite-size infinite-time limits (with corrections in $1/N_c$ and in $1/t$) have to be taken into account properly: indeed, as power laws, they present no characteristic size and time above which the corrections would be negligible. The situation is very similar to the study of the critical depinning force in driven random manifolds: the critical force presents a corrections in one over the system size [19] which has to be considered properly in order to extract its actual value. Generically, such scalings also provide a convergence criterion to the asymptotic regimes of the algorithm: one has to confirm that the CGF estimator does present corrections (first) in $1/t$ and (second) in $1/N_c$ with respect to an asymptotic value in order to ensure that such value does represent a correct evaluation of the LDF.

It would be interesting to extend our study of these scalings to systems presenting dynamical phase transitions (in the form of a non-analyticity of the CGF), where it is known that the finite-time and finite-size scalings of the CGF estimator can be very hard to overcome [9]. In particular, in this context, it would be useful to understand how the dynamical phase transition of the original system translates into anomalous features of the distribution of the CGF estimator in the cloning algorithm.

ACKNOWLEDGMENTS

E. G. thanks Khashayar Pakdaman for his support and discussions. Special thanks to the Ecuado-

rian Government and the Secretaría Nacional de Educación Superior, Ciencia, Tecnología e Innovación, SENESCYT. T. N. gratefully acknowledges the support of Fondation Sciences Mathématiques de Paris – EOTP NEMOT15RPO, PEPS LABS and LAABS Inphyniti CNRS project. V. L. acknowledges support by the National Science Foundation under Grant No. NSF PHY11-25915 during a stay at KITP, UCSB.

[1] T. Nemoto, E. Guevara Hidalgo, and V. Lecomte, arXiv:1607.04752 [cond-mat] (2016), arXiv: 1607.04752.
[2] H. Kahn and T. E. Harris, National Bureau of Standards applied mathematics series **12**, 27 (1951).
[3] F. Cérou and A. Guyader, Stochastic Analysis and Applications **25**, 417 (2007).
[4] P. G. Bolhuis, D. Chandler, C. Dellago, and P. L. Geissler, Annual Review of Physical Chemistry **53**, 291 (2002).
[5] J. Bucklew, *Introduction to Rare Event Simulation* (Springer Science & Business Media, 2013).
[6] C. Giardinà, J. Kurchan, V. Lecomte, and J. Tailleur, J. Stat. Phys. **145**, 787 (2011).
[7] C. Giardinà, Cristian, J. Kurchan, and L. Peliti, Phys. Rev. Lett. **96**, 120603 (2006).
[8] J. Tailleur and J. Kurchan, Nat Phys **3**, 203 (2007).
[9] V. Lecomte and J. Tailleur, J. Stat. Mech. **2007**, P03004 (2007).
[10] J. Tailleur and V. Lecomte, AIP Conf. Proc. **1091**, 212 (2009).
[11] P. I. Hurtado and P. L. Garrido, J. Stat. Mech. **2009**, P02032 (2009).
[12] M. Tchernookov and A. R. Dinner, J. Stat. Mech. **2010**, P02006 (2010).
[13] A. Kundu, S. Sabhapandit, and A. Dhar, Phys. Rev. E **83**, 031119 (2011).
[14] T. Nemoto, F. Bouchet, R. L. Jack, and V. Lecomte, Phys. Rev. E **93**, 062123 (2016).
[15] H. Touchette, Physics Reports **478**, 1 (2009).
[16] J. P. Garrahan, R. L. Jack, V. Lecomte, E. Pitard, K. van Duijvendijk, and F. van Wijland, J. Phys. A **42**, 075007 (2009).
[17] E. Guevara Hidalgo and V. Lecomte, J. Phys. A: Math. Theor. **49**, 205002 (2016).
[18] C. M. Rohwer, F. Angeletti, and H. Touchette, Phys. Rev. E **92**, 052104 (2015).
[19] A. B. Kolton, S. Bustingorry, E. E. Ferrero, and A. Rosso, J. Stat. Mech. **2013**, P12004 (2013).